PHYSICAL REVIEW A **73**, 022114 (2006)

Interpretational difficulties in quantum field theory

P. Krekora, Q. Su, and R. Grobe
Intense Laser Physics Theory Unit and Department of Physics, Illinois State University, Normal, Illinois 61790-4560, USA
(Received 8 August 2005; published 23 February 2006)

Based on space-time-resolved solutions to relativistic quantum field theory we illustrate interpretational difficulties in associating field-theoretical quantities with properties of particles. These difficulties are related to the fact that the definition of the spatial probability density of particles depends on the choice of the Hilbert subspace on which the field operator is projected. We illustrate these problems by analyzing pair-production probabilities and spatial densities for the electron-positron dynamics associated with a spatially localized subcritical potential that is turned on and off in time.

DOI: 10.1103/PhysRevA.73.022114 PACS number(s): 03.65.Pm

I. INTRODUCTION

"It is never hard to find trouble in field theory" [1] is just one among many statements pointing to fundamental difficulties in interpreting predictions from relativistic quantum field theory [2]. Usually these comments are based on the dissatisfaction with the inherent singularities necessary for obtaining convergent results. "You cannot neglect a quantity just because it is infinite" [3] is just another famous Dirac quote about this issue. The foreword of a valuable book by Schweber [4] contains a remark by his Ph.D. advisor, the late Bethe, in which he writes "It is always astonishing to see one's children grow up, and to find that they can do things which their parents can no longer understand. This book is a good example."

Despite the "trouble," significant progress in obtaining computational solutions to the field theoretical equations was reported in the last two decades leading to a better understanding of the electron-positron pair production observed from the collisions of heavy ions [5–8]. Numerical solutions to the single-particle Dirac equation have also been studied to explore relativistic effects in the interaction of very intense fields with single-electron systems [9–18].

Recently, we have begun to solve numerically the time-dependent Dirac equation for the electron-positron field operator. This approach has helped to illuminate a wide range of controversial questions. Some of these questions arise for complicated physical situations such as how an electron scatters off a supercritical potential barrier (Klein paradox) [19–21]. This requires the application of quantum field theory to study the combined effect of the pair-production due to the supercriticality of the potential together with the scattering at the barrier involving the Pauli principle. Other questions dealt with less complicated systems such as force-free environments. Two good examples are the mathematical phenomenon of Schrödinger's *Zitterbewegung* and the relativistic localization problem of an electron wave function [22,23]. This computational approach also permitted a first space-time-resolved study of how a bound state is formed in a supercritical and localized force field [24].

Recently it was announced [25–27] that within the next few decades new laser sources could become available that have intensities large enough to "break down" the vacuum and spontaneously produce electron-positron pairs. As this would be a first demonstration of how light can be directly converted into matter, one can expect that this program would trigger new developments that are based on quantum field theory. As more work gets devoted to obtaining a better insight into the pair-creation process with full temporal and spatial resolution, it might be beneficial to point out some of the interpretational difficulties first. We should note that the mathematical definitions of electron and positron densities do not always have a clear physical meaning.

In this paper, we will explore a challenge beyond divergences and singularities which is more fundamental and related to the problem of how to "correctly" extract physical information from mathematical electron-positron operator solutions. We analyze from two different perspectives a simple physical process of a vacuum state that is subjected to a subcritical potential for a finite time duration. We will relate the probability of electron-positron pair production to the corresponding spatial probability density of the particles. We finish with an extended discussion and speculations on the implications of these interpretational problems for future work with supercritical and also time-dependent force fields.

II. THE SPATIALLY AND TEMPORALLY DEPENDENT QUANTUM FIELD OPERATOR

Let us first briefly summarize how to obtain numerical operator solutions to the Dirac equation and refer to previous works [9,20–23] for computational details. The evolution of the quantum field operator $\hat{\Psi}(x,t)$ is governed by the Dirac equation (in atomic units),

$$i\partial_t\hat{\Psi}(x,t)=H(t)\hat{\Psi}(x,t). \tag{2.1}$$

In general, the Dirac-Hamiltonian $H(t)$ can take arbitrary forms such as $H(t)=c\alpha\,[p-A(x,t)/c]+\beta c^2+V(x,t)$, to describe the interaction of the electron-positron complex with a time-dependent electromagnetic vector field $A(x,t)$ and a scalar electric potential $V(x,t)$ [28]. To solve this equation, the operator $\hat{\Psi}$ can be expanded in the fermion creation and annihilation operators, $\hat{\Psi}(x,t)=\Sigma_p\hat{b}_p(t)w_p(x)+\Sigma_n\hat{d}_n^\dagger(t)w_n(x)$, where $w_p(x)$ and $w_n(x)$ are (four-component) orthonormal basis states. To obtain a suitable interpretation, one can

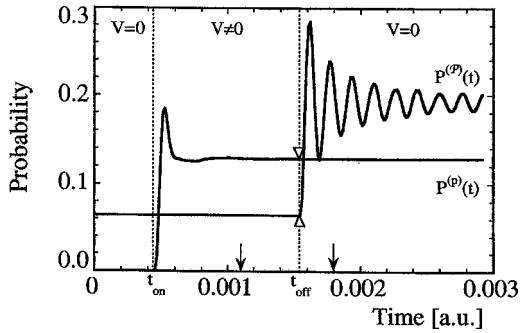

FIG. 1. The total probability of pair production $P^{(p)}(t)$ and $P^{(\mathcal{P})}(t)$ for the interaction of an initial vacuum state with a subcritical potential $V(x)$, that is abruptly turned on at t_{on} and turned off at t_{off}. $L=9.7\times10^{-2}$ a.u, $W=2.2\times10^{-3}$ a.u, $V_0=-9.38\times10^{-3}$ a.u, $t_{on}=4.56X10^{-4}$ a.u., and $t_{off}=1.37\times10^{-3}$ a.u.

choose energy eigenstates of the Dirac Hamiltonian without any interaction between upper (p) and lower (n) energies. For example, if one chooses the free-particle states, then p would label states with positive energy, $c^2 \leqslant e_p$, and n would label the negative energies, $e_n \leqslant -c^2$. We note that the completeness relation requires the upper and lower states to satisfy

$$I = \sum_p |p\rangle\langle p| + \sum_n |n\rangle\langle n| \tag{2.2}$$

where I is the identity opeator. The creation and annihilation operators evolve in time according to

$$\hat{b}_p(t) = \sum_{p'} \hat{b}_{p'}(t=0)\langle p|U(t)|p'\rangle + \sum_{n'} \hat{d}^\dagger_{n'}(t=0)\langle p|U(t)|n'\rangle, \tag{2.3a}$$

$$\hat{d}^\dagger_n(t) = \sum_{p'} \hat{b}_{p'}(t=0)\langle n|U(t)|p'\rangle + \sum_{n'} \hat{d}^\dagger_{n'}(t=0)\langle n|U(t)|n'\rangle, \tag{2.3b}$$

where the coefficients are the matrix elements of the (time-ordered) unitary propagator $U(t) \equiv \exp[-i\int_0^t dt' H(t')]$ between the states. These matrix elements are the building blocks of quantum field theory for noninteracting fermions. Each possible initial state of the entire Hilbert space needs to be evolved in time to compute all matrix elements and to obtain the field $\hat{\Psi}(x,t)$. Each state is discretized on a spatial grid and its unitary time evolution can be accomplished by a split-operator algorithm technique [9,29] that is accurate up to the fifth order in time, which with a sufficient number of temporal steps leads to fully converged results. The data presented in Fig. 1 and discussed below were obtained after a CPU time of 65 hours on an IBM P960 supercomputer cluster.

III. THE TRANSITION FROM THE QUANTUM FIELD OPERATOR TO OBSERVABLE QUANTITIES

Let us now discuss how to reduce the information contained in the mathematical operator $\hat{\Psi}(x,t)$ toward measurable quantities. In principle, the information contained in $\hat{\Psi}$ is equivalent to an infinite set of multiparticle wave functions. Given a quantum field $\hat{\Psi}(x,t)$ for the electron-positron conglomerate, the time-dependent wave function for a particular state with N electrons and M positrons can be obtained via [4]

$$\begin{aligned}\Phi(x_1,\ldots,x_N,y_1,\ldots,y_M,t) &= \langle \mathrm{vac}\|\hat{\Psi}^{(p)}(x_1,t)\cdots\hat{\Psi}^{(p)}(x_N,t)\hat{\Psi}^{(n)}_c(y_1,t)\cdots \\ &\quad\times\hat{\Psi}^{(n)}_c(y_M,t)\|\Phi(t=0)\rangle/\sqrt{(N!\,M!)}.\end{aligned} \tag{3.1}$$

Here $\|\Phi(t=0)\rangle$ denotes the initial state, and $\|\mathrm{vac}\rangle$ is the vacuum state characteristic of the particular Dirac Hamiltonian. The superscripts (p) and (n) refer to the positive energy parts of $\hat{\Psi}$ and $\hat{\Psi}_c$ which can be obtained by projecting the field on the subspaces spanned by the electron or positron states:

$$\hat{\Psi}^{(p)}(x,t) \equiv \sum_p w_p(x)\int dx' w^\dagger_p(x')\hat{\Psi}(x',t) = \sum_p \hat{b}_p(t)w_p(x), \tag{3.2a}$$

$$\begin{aligned}\hat{\Psi}^{(n)}_c(x,t) &\equiv \sum_n Cw^*_n(x)\int dx'[Cw^*_n(x')]^\dagger\hat{\Psi}_c(x',t) \\ &= \sum_n \hat{d}_n(t)Cw^*_n(x).\end{aligned} \tag{3.2b}$$

The subscript c is associated with the charge-conjugation operation. Correspondingly, $Cw^*_n(y)$ are positron states with positive energy $-e_n$ associated with the charge-conjugated Hamilton operator. One can easily convince oneself that for potentials $A(x,t)$ and $V(x,t)$ that are too weak to change the total number of particles, the wave functions based on Eq. (3.1) reduce to the solutions of the usual Dirac equation or the Schrödinger equation in the nonrelativistic limit. We thus completely recover relativistic quantum mechanics for noninteracting particles from quantum field theory [4].

The choice of the projected subspace is important with regard to the possible interpretation. We will show that the association with quantum field theoretical quantities with a "physical" particle is nontrivial inside a position- or time-dependent force field. In the simplest possible case, one can use the projection onto the force-free particle states to define the operators $\hat{\Psi}^{(p)}(x,t)$ and $\hat{\Psi}^{(n)}_c(x,t)$ associated with the Hamiltonian $c\alpha p+\beta c^2$. One would then have to interpret all quantities during the interaction as those properties that the "physical" particles would take if the interaction were *instantaneously* turned off. The last adverb is necessary to avoid any transitions due to the time dependence associated with an extended temporal turn off period. If we use below interpretive expressions such as the electron's spatial density inside the force region, they are supposed to refer to those properties the particle would have immediately after the interaction is removed.

Using the projection on the same positive energy eigenstates we can also define the total spatial density for the

electrons, $\rho^{(p)}(x,t)$, and positrons, $\rho^{(n)}(x,t)$, as

$$\rho^{(p)}(x,t) \equiv \langle \Phi(t=0) \| \hat{\Psi}^{\dagger(p)}(x,t) \hat{\Psi}^{(p)}(x,t) \| \Phi(t=0) \rangle, \tag{3.3a}$$

$$\rho^{(n)}(x,t) \equiv \langle \Phi(t=0) \| \hat{\Psi}_c^{\dagger(n)}(x,t) \hat{\Psi}_c^{(n)}(x,t) \| \Phi(t=0) \rangle. \tag{3.3b}$$

These definitions of spatial probabilities are consistent with the way the total number of particles can be computed via the sum (integral) of the occupation numbers in all electronic and positronic states:

$$\int \rho^{(p)}(x,t)dx = \sum_p \langle \Phi(t=0) \| \hat{b}_p(t)^\dagger \hat{b}_p(t) \| \Phi(t=0) \rangle, \tag{3.4a}$$

$$\int \rho^{(n)}(x,t)dx = \sum_n \langle \Phi(t=0) \| \hat{d}_n(t)^\dagger \hat{d}_n(t) \| \Phi(t=0) \rangle. \tag{3.4b}$$

IV. THE INTERACTION WITH A POTENTIAL AS A NUMERICAL ILLUSTRATION

A. Field-free perspective

So far we have defined our measurable quantities with respect to the free environment $A(x,t)=0$ and $V(x,t)=0$. In other words, if the interaction $V(x)$ were turned off instantly, all particle properties such as their spatial probabilities or expectation values would be determined correctly from the field operator.

Let us now illustrate this finding for an oversimplified system in which the state is initially in (force-free) vacuum $\|\Phi(t=0)\rangle = \|\text{vac}\rangle$ and then interacts with an electrostatic potential $V(x)$ during the time interval $t_{\text{on}} < t < t_{\text{off}}$. We choose a simple potential well [30] of the form $V(x)=V_0\{\tanh[(x+L)/W]-\tanh[(x-L)/W]\}/2$ that is characterized by two length scales. L ($=9.7\times10^{-2}$ a.u) is a measure for the extension of $V(x)$, and W ($=2.2\times10^{-3}$ a.u) is related to the width of the region where the corresponding force, proportional to the derivative $V'(x)$, is nonzero. Its shape is depicted on the bottom of Figs. 2 and 3 below. We choose $V_0=-c^2/2(=-9.4\times10^3$ a.u.) such that the lowest-lying electronic state with energy E_g is located above the lower energy continuum. Note that the energy $E_g > -c^2$ makes the potential subcritical and this property is usually identified with stable systems that do not decay spontaneously into electron-positron pairs.

In Fig. 1 we show the total pair-production probability as a function of time when viewed from a force-free perspective, defined in Eq. (3.4) as $P^{(p)}(t) \equiv \Sigma_p \langle \text{vac} \| \hat{b}_p(t)^\dagger \hat{b}_p(t) \| \text{vac} \rangle$. As the particles appear only pairwise, $P^{(p)}(t)$ is the same as $P^{(n)}(t) \equiv \Sigma_n \langle \text{vac} \| \hat{d}_n(t)^\dagger \hat{d}_n(t) \| \text{vac} \rangle$. The vertical dashed lines in the figure show the times t_{on} ($=4.56\times10^{-4}$ a.u.) and t_{off} ($=1.37\times10^{-3}$ a.u.). Let us first focus on the curve $P^{(p)}(t)$ and discuss the relevance of the second curve labeled as $P^{(\mathcal{P})}(t)$ in Sec. IV B.

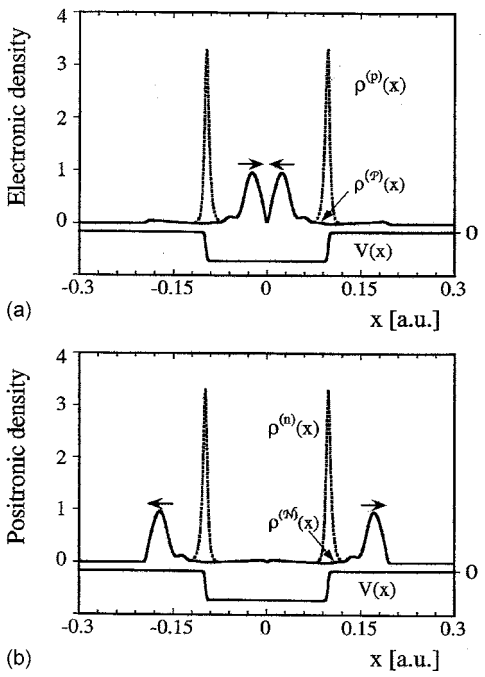

FIG. 2. The graphs on the top (a) show a snapshot of the electronic spatial probability density $\rho^{(p)}(x,t)$ and $\rho^{(\mathcal{P})}(x,t)$ taken at time $t=1.1\times10^{-3}$ a.u. (left arrow in Fig. 1) during the interaction with the potential $V(x)$ that is turned on at t_{on}. The bottom figure (b) shows the corresponding positronic densities $\rho^{(n)}(x,t)$ and $\rho^{(\mathcal{N})}(x,t)$. To set the scale we have included on the bottom the corresponding potential $V(x)$. Same parameters as in Fig. 1.

During the first time interval $t < t_{\text{on}}$, we have $P^{(p)}(t)=0$, characteristic for the nonchanging vacuum state. The rapid rise to $P^{(p)}(t) \approx 18.5\%$ around $t \approx t_{\text{on}}$ is not a numerical artifact and does not depend on any computational grid parameter. In fact, its initial growth rate is correctly predicted by first-order perturbation theory for short times $P^{(p)}(t) \approx \Sigma_p \Sigma_n |\langle n|V|p\rangle|^2 (t-t_{\text{on}})^2$ [22,31]. This early-time rise can be loosely interpreted in terms of the uncertainty product between energy and time. However, after a characteristic time (of the order $1/c^2$, $t \approx t_{\text{on}} + 5\times10^{-5}$ a.u.), $P^{(p)}(t)$ comes to a halt at $P^{(p)}(t) \approx 12.8\%$, as the potential was chosen to be subcritical and pairs can no longer be produced. Once the potential is turned off ($t > t_{\text{off}}$) this probability remains constant leaving us with the result that a subcritical potential can produce electron-positron pairs.

Even though the numerical results are exact, due to the simple nature of the instantly turned on and off interaction, we can also obtain some analytical insight. The Hamiltonian for $t_{\text{on}} < t < t_{\text{off}}$, $H = c\alpha p + \beta c^2 + V(x)$, has energy eigenstates denoted by the capital letters $H|\mathcal{P}\rangle = E_{\mathcal{P}}|\mathcal{P}\rangle$ and $H|\mathcal{N}\rangle = E_{\mathcal{N}}|\mathcal{N}\rangle$ with upper (lower) energies $E_{\mathcal{P}}$ ($E_{\mathcal{N}}$), respectively. As we chose the potential $V(x)$ to be subcritical, its energy spectrum allows a clean separation of "upper" (electronic) states with energy $E_{\mathcal{P}} \geq E_g$, and "lower" states with energy $E_{\mathcal{N}} < E_g$ that are related to (charge-conjugated) positronic states. The ground-state energy E_g denotes the eigenvalue

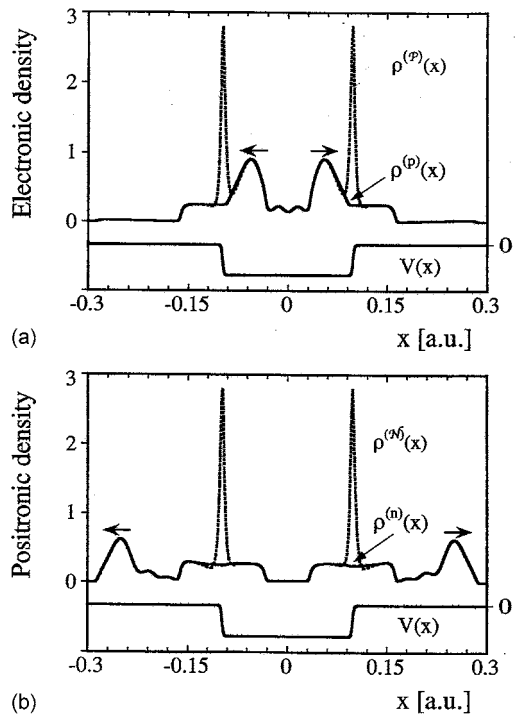

FIG. 3. The graphs on the top (a) show a snapshot of the electronic spatial probability density $\rho^{(p)}(x,t)$ and $\rho^{(\mathcal{P})}(x,t)$ taken at time $t=1.8\times10^{-3}$ a.u. (right arrow in Fig. 1) after the interaction with the subcritical potential $V(x)$. The bottom figure (b) shows the corresponding positronic densities $\rho^{(n)}(x,t)$ and $\rho^{(\mathcal{N})}(x,t)$. To set the scale we have included on the bottom the corresponding potential $V(x)$ even though it was turned off when the snapshots were taken. Same parameters as in Fig. 1.

associated with the lowest-lying normalizable state. As mentioned above, the summation over the states labeled by the small letters in Σ_p ranges from $e_p=c^2$ to ∞, whereas the summation over the capital letters $\Sigma_{\mathcal{P}}$ ranges from $E_{\mathcal{P}}=E_g$ to ∞.

The time evolution during the force-free time ($t<t_{\mathrm{on}}$) is trivial, $w_p(x,t)=\exp(-ie_pt)w_p(x)$, leading to $P^{(\mathrm{p})}(t)\equiv\Sigma_p\langle\mathrm{vac}\|\hat{b}_p(t)^\dagger\hat{b}_p(t)\|\mathrm{vac}\rangle=0$. The time evolution in $t_{\mathrm{on}}<t<t_{\mathrm{off}}$ is given by

$$\begin{aligned}\hat{b}_p(t)=&\sum_{p'}\exp(-ie_pt_{\mathrm{on}})\Bigg(\sum_{\mathcal{P}}\exp[-iE_{\mathcal{P}}(t-t_{\mathrm{on}})]\langle\mathcal{P}|p'\rangle\langle p|\mathcal{P}\rangle\\&+\sum_{\mathcal{N}}\exp[-iE_{\mathcal{N}}(t-t_{\mathrm{on}})]\langle\mathcal{N}|p'\rangle\langle p|\mathcal{N}\rangle\Bigg)\hat{b}_{p'}(t=0)\\&+\sum_{n}\exp(-ie_nt_{\mathrm{on}})\Bigg(\sum_{\mathcal{P}}\exp[-iE_{\mathcal{P}}(t-t_{\mathrm{on}})]\langle\mathcal{P}|n\rangle\langle p|\mathcal{P}\rangle\\&+\sum_{\mathcal{N}}\exp[-iE_{\mathcal{N}}(t-t_{\mathrm{on}})]\langle\mathcal{N}|n\rangle\langle p|\mathcal{N}\rangle\Bigg)\hat{d}_n^\dagger(t=0).\end{aligned}\tag{4.1}$$

If we insert this solution and the one for $\hat{b}_p^\dagger(t)$ back into the expression for $P^{(p)}(t)$ we obtain

$$\begin{aligned}P^{(p)}(t)=\sum_p\sum_n\Bigg|&\sum_{\mathcal{P}}\exp[-iE_{\mathcal{P}}(t-t_{\mathrm{on}})]\langle P|n\rangle\langle p|\mathcal{P}\rangle\\&+\sum_{\mathcal{N}}\exp[-iE_{\mathcal{N}}(t-t_{\mathrm{on}})]\langle\mathcal{N}|n\rangle\langle p|\mathcal{N}\rangle\Bigg|^2.\end{aligned}\tag{4.2}$$

As $\langle n|p\rangle=0$, this expression starts with $P^{(p)}(t)=0$ for $t\leqslant t_{\mathrm{on}}$ and then rises quickly as the complex amplitudes begin to add up as $\langle p|\mathcal{N}\rangle$ and $\langle\mathcal{P}|n\rangle$ are nonzero. As the potential $V(x)$ is finite, the unitary time evolution operator is continuous at all times and $P^{(p)}(t)$ cannot change its value in a noncontinuous way during the abrupt turn on. After most phases $E_{\mathcal{P}}(t-t_{\mathrm{on}})$ and $E_{\mathcal{N}}(t-t_{\mathrm{on}})$ have reached their maximum value, only the diagonal terms in the sum contribute, leaving us with a steady long-time value of

$$P^{(\mathrm{p})}(t)\approx\sum_p\sum_n\Bigg(\sum_{\mathcal{P}}(\langle\mathcal{P}|n\rangle\langle p|\mathcal{P}\rangle)^2+\sum_{\mathcal{N}}|\langle\mathcal{N}|n\rangle\langle p|\mathcal{N}\rangle|^2\Bigg)\tag{4.3}$$

for $t>t_{\mathrm{off}}$. These features explain from a mathematical point of view the graph $P^{(p)}(t)$ in Fig. 1. In Sec. V we will analyze the interesting spatial distribution associated with the probabilities.

B. An alternative perspective that includes the potential

One could have argued that the predictions of $\hat{\Psi}^{(p)}(x,t)$ are physically not meaningful during the time interval $t_{\mathrm{on}}<t<t_{\mathrm{off}}$ when the potential $V(x)$ is nonzero, as the very definition of the projection operation Eq. (3.2a) was based on force-free states $|p\rangle$ that have no particular relevance to this situation. We can reconsider the same physical process, however, with regard to the "correct" eigenstates $|\mathcal{P}\rangle$ and $|\mathcal{N}\rangle$ that take the potential into account. While the presentation of the field operator is of no consequence, the two subspaces $|p\rangle$ and $|\mathcal{P}\rangle$ are not identical and the corresponding scalar products between states of positive energy and states of negative energy are not necessarily zero, $\langle p|\mathcal{N}\rangle\neq0$ and $\langle\mathcal{P}|n\rangle\neq0$. As we will discuss now, this inequality will lead to difficulties in defining very fundamental quantities, such as what constitutes a physical particle and how we can count it. As the time-dependent quantum field operator is independent of what Hilbert space is used to represent it, it allows us to relate various quantities with respect to each other through Bogoliubov transformations[32]

$$\begin{aligned}\hat{\Psi}(x,t)&=\sum_p\hat{b}_p(0)w_p(x,t)+\sum_n\hat{d}_n^\dagger(0)w_n(x,t)\\&=\sum_p\hat{b}_p(t)w_p(x)+\sum_n\hat{d}_n^\dagger(t)w_n(x)\\&=\sum_{\mathcal{P}}\hat{B}_{\mathcal{P}}(0)W_{\mathcal{P}}(x,t)+\sum_{\mathcal{N}}\hat{D}_{\mathcal{N}}^\dagger(0)W_{\mathcal{N}}(x,t)\\&=\sum_{\mathcal{P}}\hat{B}_{\mathcal{P}}(t)W_{\mathcal{P}}(x)+\sum_{\mathcal{N}}(t)\hat{D}_{\mathcal{N}}^\dagger W_{\mathcal{N}}(x)\end{aligned}\tag{4.4}$$

where $\hat{B}_{\mathcal{P}}$ and $\hat{D}_{\mathcal{N}}^\dagger$ denote the electron annihilation and positron creation operators with respect to the energy eigenstates of the Dirac Hamiltonian $H=c\alpha p+\beta c^2+V(x)$ introduced in

Sec. IV A. With respect to this Hamiltonian, one would define the total number of electrons as

$$P^{(\mathcal{P})}(t) \equiv \sum_{\mathcal{P}} \langle \Phi(t=0) \| \hat{B}_{\mathcal{P}}(t)^{\dagger} \hat{B}_{\mathcal{P}}(t) \| \Phi(t=0) \rangle. \quad (4.5)$$

Note that the initial state is still $\|\Phi(t=0)\rangle = \|\text{vac}\rangle$ and not the vacuum state of H, denoted by $\|\mathcal{VAC}\rangle$. This is important as we want to describe the same physical process as before. The second graph in Fig. 1 shows the behavior of $P^{(\mathcal{P})}(t)$ during the three time intervals. It begins with a nonzero value $P^{(\mathcal{P})}(t=0) \approx 6.4\%$, which then remains constant up to time $t = t_{\text{off}}$, after which it becomes time dependent and grows to a value of $P^{(\mathcal{P})}(t) = 28.4\%$ at $t = 0.0016$ a.u., before approaching a steady value of $P^{(\mathcal{P})}(t \to \infty) = 19.2\%$. The damped oscillatory pattern is characterized by a temporal period of 1.7×10^{-4} a.u. which is remarkably close to $(2\pi)/(2c^2)$, relating it nicely to the energy gap.

The corresponding analytical solutions can be readily derived. Using the orthogonality among states of the same Hamiltonian, we can obtain from Eq. (4.4) for $t < t_{\text{on}}$:

$$\hat{B}_{\mathcal{P}}(t) = \sum_{p} \exp(-ie_p t) \langle \mathcal{P} | p \rangle \hat{b}_p(0) + \sum_{n} \exp(-ie_n t) \langle \mathcal{P} | n \rangle \hat{d}_n^{\dagger}(0) \quad (4.6)$$

which then leads to the constant but nonzero probability for $t < t_{\text{on}}$

$$P^{(\mathcal{P})}(t) = \sum_{\mathcal{P}} \sum_{n} |\langle \mathcal{P} | n \rangle|^2 \quad (4.7)$$

This initial value is nonzero as the initial state was $\|\text{vac}\rangle$, not $\|\mathcal{VAC}\rangle$, and we simply view the (unchanging) vacuum state $\|\text{vac}\rangle$ from another reference point. In Sec. V we will analyze the spatial manifestation of this nonzero probability $P^{(\mathcal{P})}(t)$ to address the question of where the corresponding "electrons" and "positrons" are located.

Next let us analyze the probability for $t \geqslant t_{\text{on}}$:

$$\hat{B}_{\mathcal{P}}(t) = \exp[-iE_{\mathcal{P}}(t - t_{\text{on}})] \left(\sum_{p} \exp(-ie_p t_{\text{on}}) \langle \mathcal{P} | p \rangle \hat{b}_p(0) + \sum_{n} \exp(-ie_n t_{\text{on}}) \langle \mathcal{P} | n \rangle d_n^{\dagger}(0) \right) \quad (4.8)$$

which yields the result for $t_{\text{on}} < t < t_{\text{off}}$

$$P^{(\mathcal{P})}(t) = \sum_{\mathcal{P}} \sum_{n} |\langle \mathcal{P} | n \rangle|^2. \quad (4.9)$$

This time-independence character is expected as we chose the "correct" eigenbasis for this period of interaction and any transitions among the energy eigenstates are not possible. Once the potential is turned off, however, $P^{(\mathcal{P})}(t)$ loses its meaning as the true particle probability and its value grows to more than 28.4%, before it settles to a stationary value close to 19.2%.

This remarkable growth after $t = t_{\text{off}}$ can be related to the turn-off burst discovered by Haan and his collaborators in 1997 [33,34] in numerical studies of near-threshold photoionization. In his case, a dressed bound state created by the laser field collapses when the laser field is relatively abruptly turned off and the atomic-continuum portion of this state is free to escape to infinity leading to an additional bump in the probability density of the escaping electron. This effect is quite universal and was later observed also numerically in the context of atoms with two active electrons [35].

V. SPATIAL MANIFESTATION OF THE DIFFERENCE BETWEEN $P^{(p)}(t)$ AND $P^{(\mathcal{P})}(t)$

Let us now illuminate the pair-production probabilities $P^{(p)}(t)$ and $P^{(\mathcal{P})}(t)$ by analyzing their spatial densities. The physical state of the electron-positron complex is described by the time-dependent field operator $\hat{\Psi}(x,t)$; however, the positive frequency part of it depends on the coordinate system characterized by the chosen basis states:

$$\hat{\Psi}^{(p)}(x,t) \equiv \sum_{p} w_p(x) \int dx' w_p^{\dagger}(x') \hat{\Psi}(x',t) = \sum_{p} \hat{b}_p(t) w_p(x), \quad (5.1a)$$

$$\hat{\Psi}_c^{(n)}(x,t) \equiv \sum_{n} C w_n^*(x) \int dx' [C w_n^*(x')]^{\dagger} \hat{\Psi}_c(x',t) = \sum_{n} d_n(t) C w_n^*(x), \quad (5.1b)$$

$$\hat{\Psi}^{(\mathcal{P})}(x,t) \equiv \sum_{\mathcal{P}} W_{\mathcal{P}}(x) \int dx' W_{\mathcal{P}}^{\dagger}(x') \hat{\Psi}(x',t) = \sum_{\mathcal{P}} B_{\mathcal{P}}(t) W_{\mathcal{P}}(x), \quad (5.1c)$$

$$\hat{\Psi}_c^{(\mathcal{N})}(x,t) \equiv \sum_{\mathcal{N}} C W_{\mathcal{N}}^*(x) \int dx' [C W_{\mathcal{N}}^*(x')]^{\dagger} \hat{\Psi}_c(x',t) = \sum_{\mathcal{N}} D_{\mathcal{N}}(t) C W_{\mathcal{N}}^*(x). \quad (5.1d)$$

These four definitions lead to the corresponding spatial densities:

$$\rho^{(p)}(x,t) \equiv \langle \Phi(t=0) \| \hat{\Psi}^{\dagger(p)}(x,t) \hat{\Psi}^{(p)}(x,t) \| \Phi(t=0) \rangle, \quad (5.2a)$$

$$\rho^{(n)}(x,t) \equiv \langle \Phi(t=0) \| \hat{\Psi}_c^{\dagger(n)}(x,t) \hat{\Psi}_c^{(n)}(x,t) \| \Phi(t=0) \rangle, \quad (5.2b)$$

$$\rho^{(\mathcal{P})}(x,t) \equiv \langle \Phi(t=0) \| \hat{\Psi}^{\dagger(\mathcal{P})}(x,t) \hat{\Psi}^{(\mathcal{P})}(x,t) \| \Phi(t=0) \rangle, \quad (5.2c)$$

$$\rho^{(\mathcal{N})}(x,t) \equiv \langle \Phi(t=0) \| \hat{\Psi}_c^{\dagger(\mathcal{N})}(x,t) \hat{\Psi}_c^{(\mathcal{N})}(x,t) \| \Phi(t=0) \rangle. \quad (5.2d)$$

It should be obvious that $\hat{\Psi}^{(p)}(x,t) \neq \hat{\Psi}^{(\mathcal{P})}(x,t)$, if $\langle \mathcal{P} | n \rangle$ or $\langle \mathcal{N} | p \rangle$ is nonzero and the corresponding positive and nega-

tive subspaces with and without the potential overlap.

The discussion below will show that the spatial densities permit a clear classification of two distinct spatial regions. The first region is characterized by *reference-frame-dependent* densities for which $\rho^{(p)}(x,t) \neq \rho^{(\mathcal{P})}(x,t)$ and $\rho^{(n)}(x,t) \neq \rho^{(\mathcal{N})}(x,t)$. This region refers to those locations for which the force associated with the atomic potential $[\approx V'(x)]$ is nonzero. In our particular example this corresponds to the spatial turn on and off regions $-W/2-L<x<-L+W/2$ and $-W/2+L<x<L+W/2$. In temporal regimes $t<t_{\mathrm{on}}$ and $t>t_{\mathrm{off}}$ where the potential $V(x)$ is not present, $\rho^{(p)}(x,t)$ is the true electronic spatial probability density, whereas $\rho^{(\mathcal{P})}(x,t)$ describes the electrons' correct density for the remaining times $t_{\mathrm{on}}<t<t_{\mathrm{off}}$, when the potential is turned on. The second region consists of locations where the force is nearly zero, $V'(x)\approx 0$, characteristic of $x<-L-W/2$, $W/2-L<x<L-W/2$ and $L+W/2<x$. In these spatial regions the probability density *does not depend on* the choice of reference frame, i.e., $\rho^{(p)}(x,t)=\rho^{(\mathcal{P})}(x,t)$ and $\rho^{(n)}(x,t)=\rho^{(\mathcal{N})}(x,t)$ and the interpretation in terms of real particles is unambiguous.

Let us discuss first the spatial probability density based on force-free states for the electron $\rho^{(\mathrm{p})}(x,t)$ [Figs. 2(a) and 3(a)] and the positron $\rho^{(n)}(x,t)$ [Figs. 2(b) and 3(b)]. Figure 2 was taken at time $t=1.14\times 10^{-3}$ a.u. when the potential was on ($t_{\mathrm{on}}<t<t_{\mathrm{off}}$) and Fig. 3 corresponds to the densities after the potential has been turned off at $t=1.82\times 10^{-3}$ a.u. as marked by arrows in Fig. 1.

Let us first analyze the evolution of the electronic portion $\rho^{(\mathrm{p})}(x,t)$ shown by the dashed line in Fig. 2(a). For times $t<t_{\mathrm{on}}$ we have $\rho^{(\mathrm{p})}(x,t)=0$, but for the second time regime $t>t_{\mathrm{on}}$ we observe an initial growth of probability at the two regions around $x=\pm L$ (± 0.097 a.u.), where $V'(x)$ is nonzero. At time $t=1.14\times 10^{-3}$ a.u. the density (of total area 12.8%) can be characterized by three parts.

One part of the electronic distribution remains "stuck" at these wings of the potential at $x=\pm L$. In this paper, we propose to call the associated states "ghost states." In the presence of the force these particular states may not be interpreted as physical probabilities of real particles, For example, a real electron would be repelled by the left edge to the right. As the two "unphysical" peaks are relatively isolated from the real densities, these ghost states can be loosely associated with a total weight of 6.4%, defined as $\int dx\, \rho^{(p)}(x,t)$, where the integration covers the particular region, here from $x=-0,12$ to -0.074 a.u. and from 0.074 to 0.12 a.u.

A second part of this density moves inward and then oscillates back and forth between the turning points $x=\pm L$ while spreading. The two peaks move through each other and have weight of 6.0% when the snapshot was taken and must be interpreted as a "real" electron as we see below.

A third and minute part of $\rho^{(\mathrm{p})}(x)$ ($\approx 0.4\%$) is ejected to $\pm\infty$ as discussed above. This portion can be loosely associated with the very early-time behavior and the energy-time uncertainty relation. In the snapshot in Fig. 2(a), this particular portion has reached $x\approx\pm 0.19$ a.u. Once ejected, these early electrons cannot turn around and return back to the potential region.

Let us now compare the data for $\rho^{(p)}(x,t)$ with the true electron probability density in this temporal region obtained from the "correct" projection leading to $\rho^{(\mathcal{P})}(x,t)$ and shown by the solid line in Fig. 2(a). The two probabilities agree everywhere in the force-free regions. The unphysical ghost states predicted by the mathematical quantity $\rho^{(p)}(x,t)$, however, are entirely absent in this "correct" reference frame. Comparing Figs. 2(a) and 2(b) we also note that the electronic and positronic ghost states are similar, in this particular region, showing that also the ghost states occur in pairs.

Figure 2(b) compares the two corresponding densities $\rho^{(n)}(x,t)$ and $\rho^{(\mathcal{N})}(x,t)$ for the positrons. The two large peaks at $x\approx\pm 0.172$ a.u. with a weight of 6.0% show the outgoing ejected positron density, whereas the two peaks at $x\approx\pm 0.097$ a.u. in $\rho^{(n)}(x,t)$ are positronic ghost states that have no counterpart in $\rho^{(\mathcal{N})}(x,t)$. The small distribution (with weight 0.4%) inside the potential [where $\rho^{(n)}(x,t)$ and $\rho^{(\mathcal{N})}(x,t)$ agree] corresponds directly to the positrons that have accompanied the early (energy-time-uncertainty "triggered") electron mentioned above.

Comparing the norm of various portions of the densities with the probabilities discussed in Sec. II makes a direct identification now possible. The rise of $P^{(p)}(t)$ to 12.8% corresponds to 0.4% for the early ejected electron, 6.0% is for the bound electron, and 6.4% is associated with the ghost states. On the other hand, the constant probability $P^{(\mathcal{P})}(t)$ of 6.4% amounts to 0.4% for the early ejected electron and 6.0% of the bound electron. As a side remark, we should note that for $t<t_{\mathrm{on}}$, the nonzero distribution for $P^{(\mathcal{P})}(t)\approx 6.4\%$ corresponds entirely to ghost states located in the force region where $V'(x)\neq 0$.

The interesting interplay between ghost and real states in the two reference frame projections continues for the third temporal region where the potential is turned off. In Fig. 3 we display the corresponding densities for $t=1.82\times 10^{-3}$ a.u. The two electronic peaks in Fig. 3(a) associated with the arrows are now free to escape, together with the ghost states which have become real electrons and positrons moving in $\pm x$ directions. At $x=\pm L$, where the force was maximum before it was turned off, additional snapshots [36] indicate that the maxima of the electronic and positronic ghost states oscillate in time, directly responsible for the oscillatory probability $P^{(\mathcal{P})}(t)$ shown in Fig. 1 for $t>t_{\mathrm{off}}$. The two main peaks at $x=\pm 0.25$ a.u, in Fig, 3(b) represent the escaping positron probability. Its center has moved from $x=\pm 0.172$ a.u. [Fig. 2(b) for $t=1.14\times 10^{-3}$ a.u.] to $x=\pm 0.251$ a.u. [Fig. 3(b) for $t=1.82\times 10^{-3}$ a.u.] suggesting a center velocity of 116 a.u. corresponding to an energy exceeding that of the potential barrier.

VI. DISCUSSION

In summary, we examined the pair-production process due to an instantly turned on and off subcritical potential. For our choice of parameters, we observed a final pair-production probability of 12.8%. The corresponding spatial densities permit a clear interpretation of this amount, consisting of 6% of positrons that were ejected by the force directly

after the turn on, 0.4% of positrons that were ejected toward the inside of the potential, and another portion of 6.4% that was released after the potential has been turned off. This process was monitored from two different reference frames. The very definition of what one could call an electron or positron depends on the choice for the corresponding Hilbert subspace on which the electron-positron field operator is projected. In the absence of any interaction, the positive energy subspace spanned by the force-free states seems to be the natural choice and the quantity $P^{(p)}(t)$ is the true probability for pair production. However, for situations in which a potential is turned on, the subspace spanned by the upper-energy eigenstates is more suitable and the quantity $P^{(\mathcal{P})}(t)$ defined in Eq. (4.5) should be interpreted as the physical probability of real particles.

Following this reasoning we can now describe the most important observation in this work concerning an unavoidable "discontinuity" when the frame of reference is switched during the turn off moment at $t=t_{\mathrm{off}}$. Figure 1 showed that $P^{(\mathcal{P})}(t_{\mathrm{off}})=6.4\%$ whereas $P^{(p)}(t_{\mathrm{off}})=12.8\%$ as emphasized by the two triangles in the graphs. In each temporal region one definition is unambiguously identifiable with the corresponding particle probability. However, the two probabilities do not continuously go over into each other at $t=t_{\mathrm{off}}$ due to the required sudden change of perspective. It appears that the very existence of a particle (or at least its probability for existence) can change instantly if the reference frame has to be changed instantly associated with an abruptly removed external force field. We have seen that spatial manifestations of the required continuity in the evolution leads to the occurrence of the ghost states.

An additional comment about the abruptness of this change is in order. Physically, a particle cannot appear instantly and requires a time of at least $1/c^2$ for its creation [37] as shown by Fig. 1. It is therefore incorrect to interpret the jump mentioned above as an instantaneous production of particles during the very turn-off moment. The continuity of the time-evolution operator prohibits any finite pair production during a time interval of zero duration as the potential's strength and its corresponding force is finite. This leaves us with a very unsatisfactory status of our present understanding of quantum field theory or elementary particle physics.

From a practical point of view, does this mean that the counting rate at a particle detector would change instantly at times t_{on} and t_{off}? Every physical detector measures only a particular physical property of a particle (spin, position, velocity, etc.) and then infers from that information about the very existence of a particle. Similarly, our theoretical "detectors" leading to $P^{(p)}(t)$ and $P^{(\mathcal{P})}(t)$ basically measure the particle's energy by counting the occupation numbers with regard to force-free and force-containing energy states, respectively. As these two energies are different, the corresponding particle counting rates are different as well. Each detector, however, would provide a continuous counting signal even during the turn-on and -off periods of the potential. In order to further examine the particular role of the detection device, one could also couple a simple model system such as a harmonic oscillator to our dynamics and define the localization properties in terms of transition probabilities of the detector.

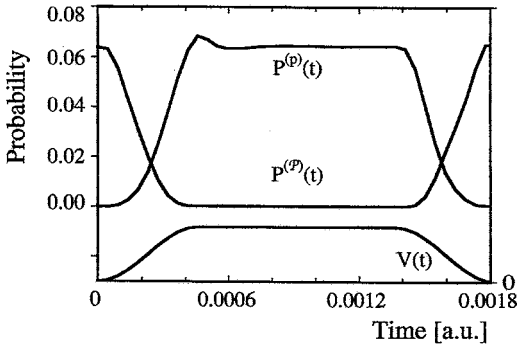

FIG. 4. The total probability of pair production $P^{(p)}(t)$ and $P^{(\mathcal{P})}(t)$ for the interaction of an initial vacuum state with a subcritical potential $V(x)$, that is adiabatically turned on and off as shown by the bottom graph labeled $V(t)$. Same parameters as in Fig. 1.

The ghost states exist in spatial regions where the force is nonzero and their evolution seems to be inconsistent with that of a true negatively or positively charged particle. One may wonder how it is possible at all to generate mathematically an electronic ghost wave function that consists via definition entirely of force-free states $w_p(x)$ with positive energy but does not evolve like a real electron in a force field. This interesting question, however, is partially ill defined. The ghost densities in $\rho^{(p)}(x,t)$ and $\rho^{(n)}(x,t)$ are similar, and each of them cannot be described individually by a (coherent) single-particle wave function. In fact, ghost states can only be described by a fully entangled two-particle wave function that does not factorize into two independent states. A density is the only single-particle description available for ghost states. Once the force field is removed, the ghost states correspond immediately to real particle densities.

At the end of Sec. IV we have discussed the similarity between the turn-off burst discovered by Haan *et al.* [33,34] and our increase of $P^{(\mathcal{P})}(t)$ after t_{off}. We should remark that the Haan effect occurs in nonrelativistic quantum mechanics where the spatial density is given by the absolute square of the wave function which does not depend on the choice of basis states for its representation. The relativistic case discussed in this work is more complicated due to the incompleteness of the subspace with positive energy, the densities depend on the basis states and a direct association of Haan's field-dressed states with our ghost states is nontrivial.

It seems that according to the definition of $P^{(p)}(t)$ (which instantly becomes the correct definition once the potential is turned off), even a subcritical potential can produce permanent pairs for a finite amount of time in those spatial regions, where its associated force is nonzero. In order to show that these pairs can be avoided if a subcritical potential is turned on and off slowly enough, we have repeated the simulation leading to the data in Figs. 2 and 3 for the nearly adiabatic case. To set the scale, the bottom graph in Fig. 4 shows the time dependence of the potential which was turned on and off with a temporal amplitude given by a sine-squared function. The two curves correspond again to $P^{(p)}(t)$ and $P^{(\mathcal{P})}(t)$, respectively. We see that while $P^{(\mathcal{P})}(t)$ reduces from its initial value of 6.4% to zero after the turn on, $P^{(p)}(t)$ grows to 6.4% but then reduces to nearly zero once the potential is turned

off, supporting the fact that under adiabatic conditions a subcritical potential cannot produce pairs. A probability $P^{[\mathcal{P}(t)]}(t)$ that would be computed from the projection on the instantaneous positive energy eigenstates of $H(t)$ at each instant in time, would be constant $P^{[\mathcal{P}(t)]}(t)=0$ under adiabatic conditions. The rise in $P^{(P)}(t)$ to 6.4% also shows that ghost states appear regardless of the particular shape of the turn on of the potential. However, the way the force field is turned off is more relevant. For an abrupt turn off the ghosts become real particles as we showed in Fig. 3, but they "annihilate" for an adiabatic turn off as shown in Fig. 4.

The importance of the appropriate choice of basis states has already been commented on and is related to the in-out state formalism traditionally used in S-matrix calculations [5]. In our present situation, each definition is unambiguous even during the interaction with a subcritical potential. An additional complication, however, is unavoidable if the system were supercritical. As often discussed in the context of relativistic collisions of heavy nuclei, the potential $V(x)$ can be so deep, that the energy of the lowest-lying bound state is below $-c^2$, in other words, the ground state "dives" into the lower-energy continuum. As a result the system is no longer stable; the vacuum can "break down" and electron-positron pairs are produced. For a Dirac Hamiltonian with a supercritical potential the energy levels can no longer be categorized by their energy alone into "upper" (electronic) and "lower" (positronic) energy spaces and an interpretation of the quantities inside such a potential region becomes truly problematic.

Yet an additional complication occurs if we want to study laser-induced supercriticality as mentioned in the Introduction. In this case, pairs can be produced due to the time dependence of the external laser field as well as due to the (possibly) supercritical strength of the force field itself. As it is highly desired to monitor the temporal and spatial evolution of the particles during their creation and interaction with the fields, serious conceptual problems in interpreting the mathematical quantities need to be addressed.

The present analysis was based on numerical solutions to the Dirac equation for the Sauter potential. We should mention that other one-dimensional potentials, such as the Woods-Saxon potential, e.g., permit analytical scattering solutions [38], and would allow a similar discussion also for the case of the Klein-Gordon equation. Even though the detailed behavior of supercritical Dirac [39] and Klein-Gordon states is different, the corresponding transmission profiles can have similar structure.

We should finally remark that in order to remain focused on the interpretational difficulties we purposely used an oversimplified model system. It was restricted to one spatial dimension, and a real temporally turned on electric field would also trigger a magnetic field that is excluded in our discussion. Due to causality a truly instantaneous turned-on field is not possible, but the interpretational difficulties are more universal. Also the description of the interaction of particles with an external field is just an approximation and a more correct approach would involve true photon-particle interactions that are presently beyond computational feasibility for us.

ACKNOWLEDGMENTS

This work has been supported by the NSF under Grant No. PHY-0456790. We have enjoyed several discussions with Professors I. Bialynicki-Birula, M. V. Fedorov, C. C. Gerry, S. L. Haan, and H. R. Reiss. We also acknowledge support from the Research Corporation and NCSA for supercomputing time.

[1] See J. D. Bjorken and S. D. Drell, *Relativistic Quantum Fields* (McGraw-Hill, New York, 1965), Sec. 15.5.
[2] E. M. Henley and W. Thirring, *Elementary Quantum Field Theory* (McGraw-Hill, New York, 1962).
[3] P. A.M. Dirac, H. Hora, and J. R. Shepanski, *Directions in Physics* (Wiley, New York, 1978).
[4] S. S. Schweber, *An Introduction to Relativistic Quantum Field Theory* (Harper & Row, New York, 1962).
[5] W. Greiner, B. Müller, and J. Rafelski, *Quantum Electrodynamics of Strong Fields* (Springer-Verlag, Berlin, 1985).
[6] K. Momberger, N. Grün, and W. Scheid, Z. Phys. D: At., Mol. Clusters **18**, 133 (1991).
[7] J. C. Wells, V. E. Oberacker, M. R. Strayer, and A. S. Umar, Nucl. Instrum. Methods Phys. Res. B **99**, 293 (1995).
[8] A. Belkacem, H. Gould, B. Feinberg, R. Bossingham, and W. E. Meyerhof, Phys. Rev. A **56**, 2806 (1997).
[9] J. W. Braun, Q. Su, and R. Grobe, Phys. Rev. A **59**, 604 (1999).
[10] U. W. Rathe, P. Sanders, and P. L. Knight, Parallel Comput. **25**, 525 (1999).
[11] R. E. Wagner, Q. Su, and R. Grobe, Phys. Rev. Lett. **84**, 3282 (2000).
[12] J. S. Roman, L. Roso, and H. R. Reiss, J. Phys. B **33**, 1869 (2000).
[13] R. E. Wagner, P. J. Peverly, Q. Su, and R. Grobe, Phys. Rev. A **61**, 035402 (2000).
[14] P. Krekora, R. E Wagner, Q. Su, and R. Grobe, Phys. Rev. A **63**, 025404 (2001).
[15] C. H. Keitel, Contemp. Phys. **42**, 353 (2001).
[16] P. Krekora, Q. Su, and R. Grobe, J. Phys. B **34**, 2795 (2001).
[17] A. Maquet and R. Grobe, J. Mod. Opt. **49**, 2001 (2002).
[18] P. Krekora, Q. Su, and R. Grobe, Phys. Rev. A **66**, 013405 (2002).
[19] N. Dombey and A. Calogeracos, Phys. Rep. **315**, 41 (1999).
[20] P. Krekora, Q. Su, and R. Grobe, Phys. Rev. Lett. **92**, 040406 (2004).
[21] P. Krekora, Q. Su, and R. Grobe, Phys. Rev. A **72**, 064103 (2005).
[22] P. Krekora, Q. Su, and R. Grobe, Phys. Rev. Lett. **93**, 043004 (2004).
[23] P. Krekora, Q. Su, and R. Grobe, Phys. Rev. A **70**, 054101 (2004).

[24] P. Krekora, K. Cooley, Q. Su, and R. Grobe, Phys. Rev. Lett. **95**, 070403 (2005).
[25] D. P. Umstadter, C. Barty, M. Perry, and G. A. Mourou, Opt. Photonics News **9**, 41 (1998).
[26] G. A. Mourou, C. P. J. Barty, and M. D. Perry, Phys. Today **51** (1), 22 (1998).
[27] G. A. Mourou and V. Yanovsky, Opt. Photonics News **15**, 40 (2004).
[28] B. Thaller, *The Dirac Equation* (Springer, Berlin, 1992).
[29] A. D. Bandrauk and H. Shen, J. Phys. A **27**, 7147 (1994).
[30] F. Sauter, Z. Phys. **69**, 742 (1931); **73**, 547 (1931).
[31] P. Krekora, K. Cooley, Q. Su, and R. Grobe, Laser Phys. **15**, 282 (2005).
[32] B. R. Holstein, Am. J. Phys. **66**, 507 (1998).
[33] S. L. Haan, B. Langdon, D. Streuker, and H. Nymeyer, Laser Phys. **7**, 115 (1997).
[34] S. L. Haan, E. Hamilton, and B. Langdon, Laser Phys. **7**, 892 (1997).
[35] S. L. Haan and R. Grobe, Laser Phys. **8**, 885 (1998).
[36] For a computer animated movie see www.phy.ilstu.edu/ILP
[37] P. Krekora, Q. Su, and R. Grobe, J. Mod. Opt. **52**, 489 (2005).
[38] C. Rojas and V. M. Villalba, Phys. Rev. A **71**, 052101 (2005).
[39] V. S. Popov, Sov. Phys. JETP **32**, 526 (1971).